SUPPLEMENTARY DATA

TRIM7 ubiquitinates SARS-CoV-2 membrane protein to limit apoptosis and viral replication

Maria Gonzalez-Orozco[1], Hsiang-chi Tseng[2], Adam Hage[1], Hongjie Xia[3], Padmanava Behera[2], Kazi Afreen[2], Yoatzin Peñaflor-Tellez[2], Maria I. Giraldo[1], Matthew Huante[1], Lucinda Puebla-Clark[4], Sarah van Tol[1], Abby Odle[2], Matthew Crown[5], Natalia Teruel[6], Thomas R Shelite[4], Vineet Menachery[1], Mark Endsley[1], Janice J. Endsley[1], Rafael J. Najmanovich[6], Matthew Bashton[5], Robin Stephens[4,7], Pei-Yong Shi[3], Xuping Xie[3], Alexander N. Freiberg[8], Ricardo Rajsbaum[1,2,*]

Author affiliations and footnotes

[1]Department of Microbiology and Immunology, University of Texas Medical Branch, Galveston, TX

[2]Center for Virus-Host-Innate-Immunity, RBHS Institute for Infectious and Inflammatory Diseases, and Department of Medicine, New Jersey Medical School, Rutgers University, Newark, NJ

[3]Department of Biochemistry and Molecular Biology, University of Texas Medical Branch, Galveston, TX

[4]Department of Internal Medicine, Division of Infectious Diseases, University of Texas Medical Branch, Galveston, TX

[5]Hub for Biotechnology in the Built Environment, Department of Applied Sciences, Faculty of Health and Life Sciences, Northumbria University, Newcastle, UK

[6]Department of Pharmacology and Physiology, Faculty of Medicine, Université de Montréal, Montreal, Canada

[7]Center for Immunity and Inflammation and Department of Pharmacology, Physiology and Neuroscience, New Jersey Medical School, Rutgers University, Newark, NJ

[8]Department of Pathology, University of Texas Medical Branch, Galveston, TX

[*]Corresponding author: ricardo.rajsbaum@rutgers.edu

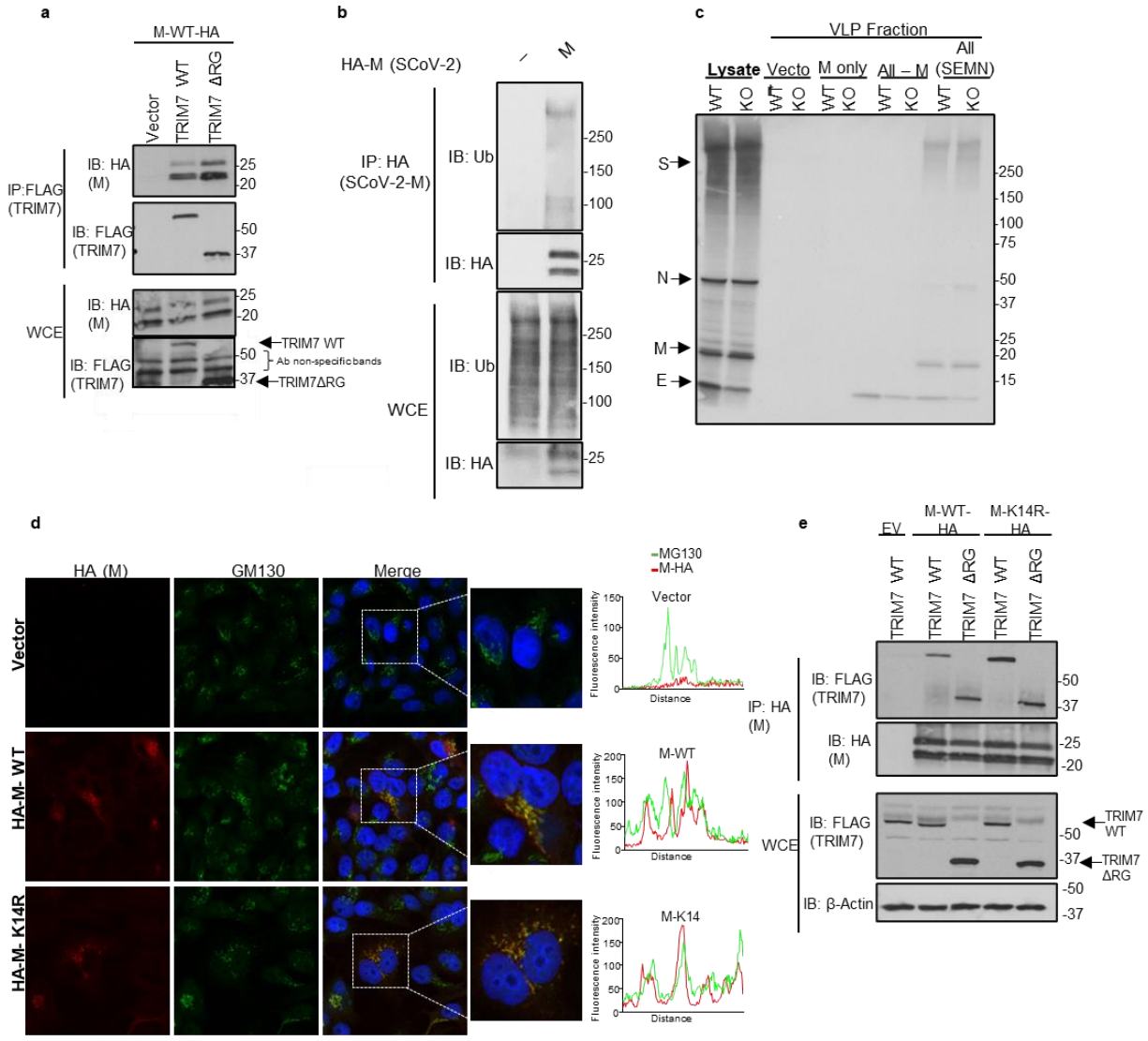

Figure S1. Ubiquitination of M by TRIM7 does not affect budding. HEK 293T cells transfected with a) 200ng or TRIM7 WT or ΔRG-FLAG and 100ng of M-HA and immunoprecipitated with FLAG beads. b) 200ng of M-HA and immunoprecipitated using HA beads c) VLPs in supernatant released by A549 WT and TRIM7 KO cells (KO). d, Confocal microscopy of Hela cells expressing M-WT-HA or M-K14R-HA (Red) and label with anti-MG130 (Golgi Marker) for 24 hours. Colocalization profile bottom show the fluorescence intensity. e) 200ng or TRIM7 WT or ΔRG-FLAG and 100ng of M-HA (WT or K14R) and immunoprecipitated with HA beads. Representative experiments of at least 2 independent experiments

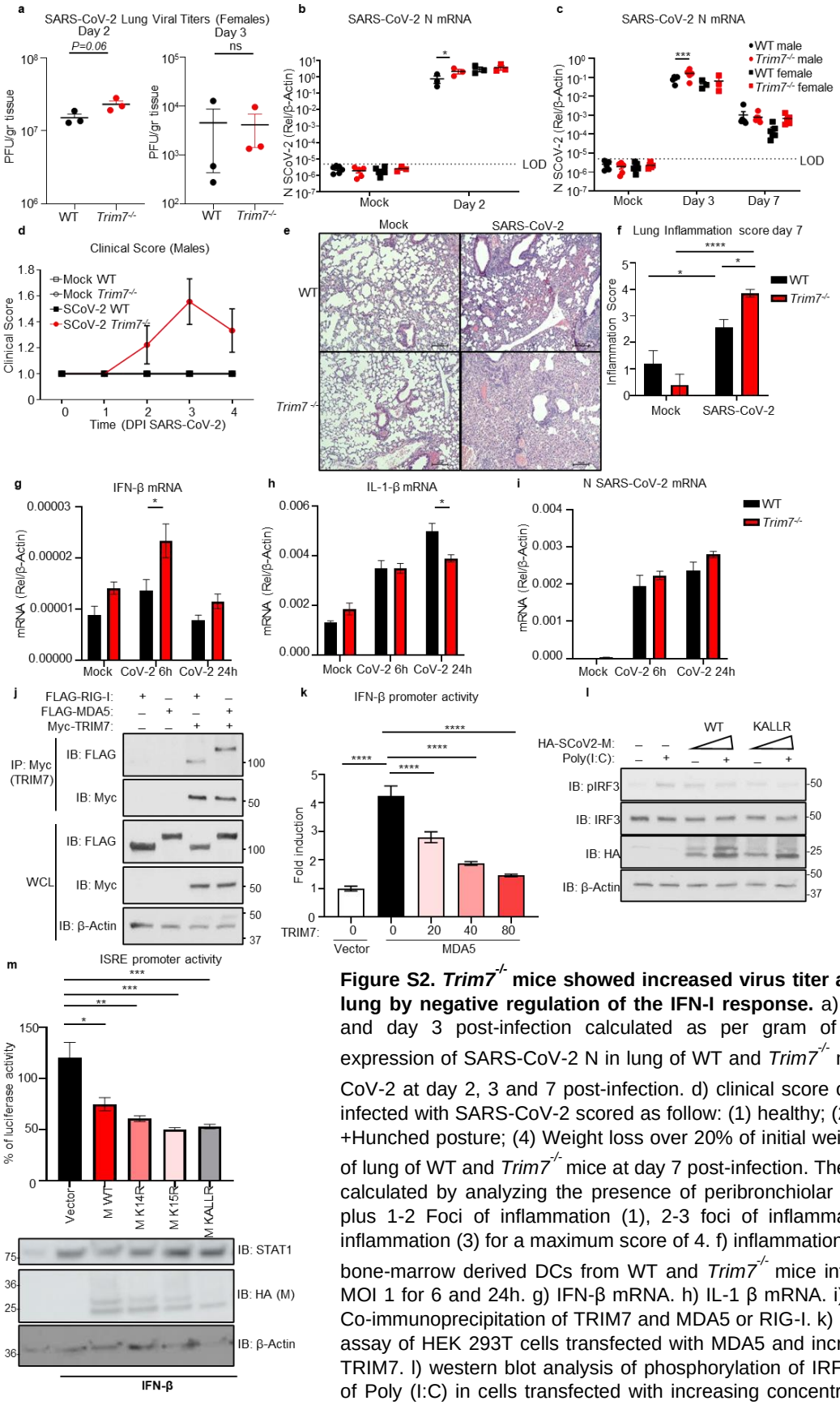

Figure S2. *Trim7*$^{-/-}$ mice showed increased virus titer and inflammation in the lung by negative regulation of the IFN-I response. a) lung viral titers at day 2 and day 3 post-infection calculated as per gram of tissue. b-c) viral RNA expression of SARS-CoV-2 N in lung of WT and *Trim7*$^{-/-}$ mice infected with SARS-CoV-2 at day 2, 3 and 7 post-infection. d) clinical score of WT and *Trim7*$^{-/-}$ males infected with SARS-CoV-2 scored as follow: (1) healthy; (2) Ruffled fur; (3) score 2 +Hunched posture; (4) Weight loss over 20% of initial weight. e) histology analysis of lung of WT and *Trim7*$^{-/-}$ mice at day 7 post-infection. The inflammatory score was calculated by analyzing the presence of peribronchiolar infiltrates (Yes=1, No=0) plus 1-2 Foci of inflammation (1), 2-3 foci of inflammation (2) and 3+ foci of inflammation (3) for a maximum score of 4. f) inflammation score. qPCR analysis of bone-marrow derived DCs from WT and *Trim7*$^{-/-}$ mice infected with SARS-CoV-2 MOI 1 for 6 and 24h. g) IFN-β mRNA. h) IL-1 β mRNA. i) N SARS-CoV-2 RNA. j) Co-immunoprecipitation of TRIM7 and MDA5 or RIG-I. k) IFN-β Luciferase reporter assay of HEK 293T cells transfected with MDA5 and increasing concentrations of TRIM7. l) western blot analysis of phosphorylation of IRF3 induced by stimulation of Poly (I:C) in cells transfected with increasing concentrations of M-WT or KallR mutant. m) ISRE luciferase reporter assay of cells transfected with M-WT or mutants K14R, K15R or KallR stimulated with IFN- β for 24h. Data are depicted as Mean ±SEM. T-test analysis, one-way or 2-way Tukey's multiple comparisons tests. $p < 0.001$ **, $p < 0.0001$ ***, $p < 0.00001$ ****.

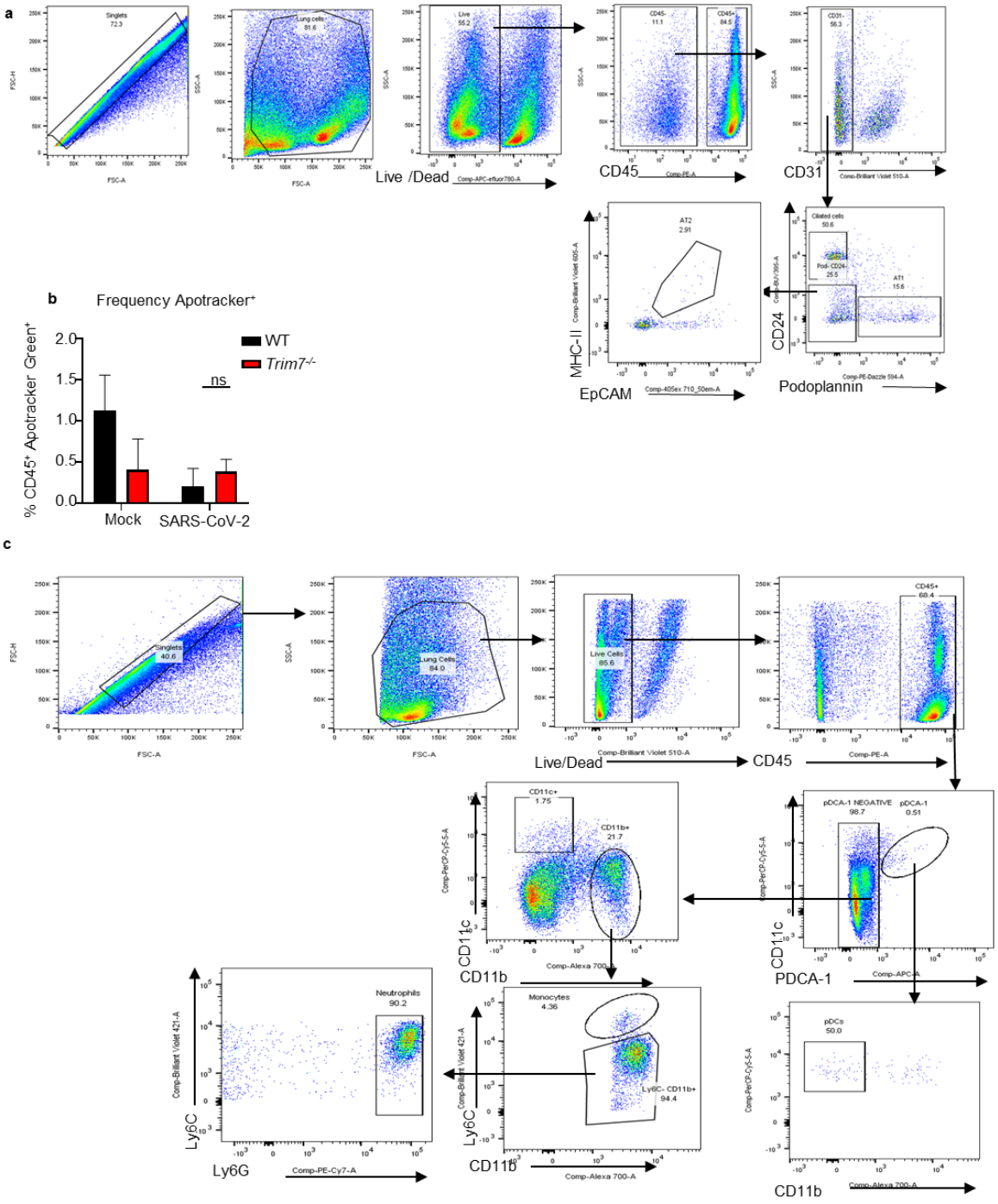

Figure S3. Flow cytometry gating strategy. a) flow cytometry gating strategy for lung epithelial cells. b) frequency of cells CD45^{+} Apotracker^{+} in lung of mice infected with SARS-CoV-2 at day 3 post-infection. c) gating strategy for flow cytometry analysis of innate immune cells.

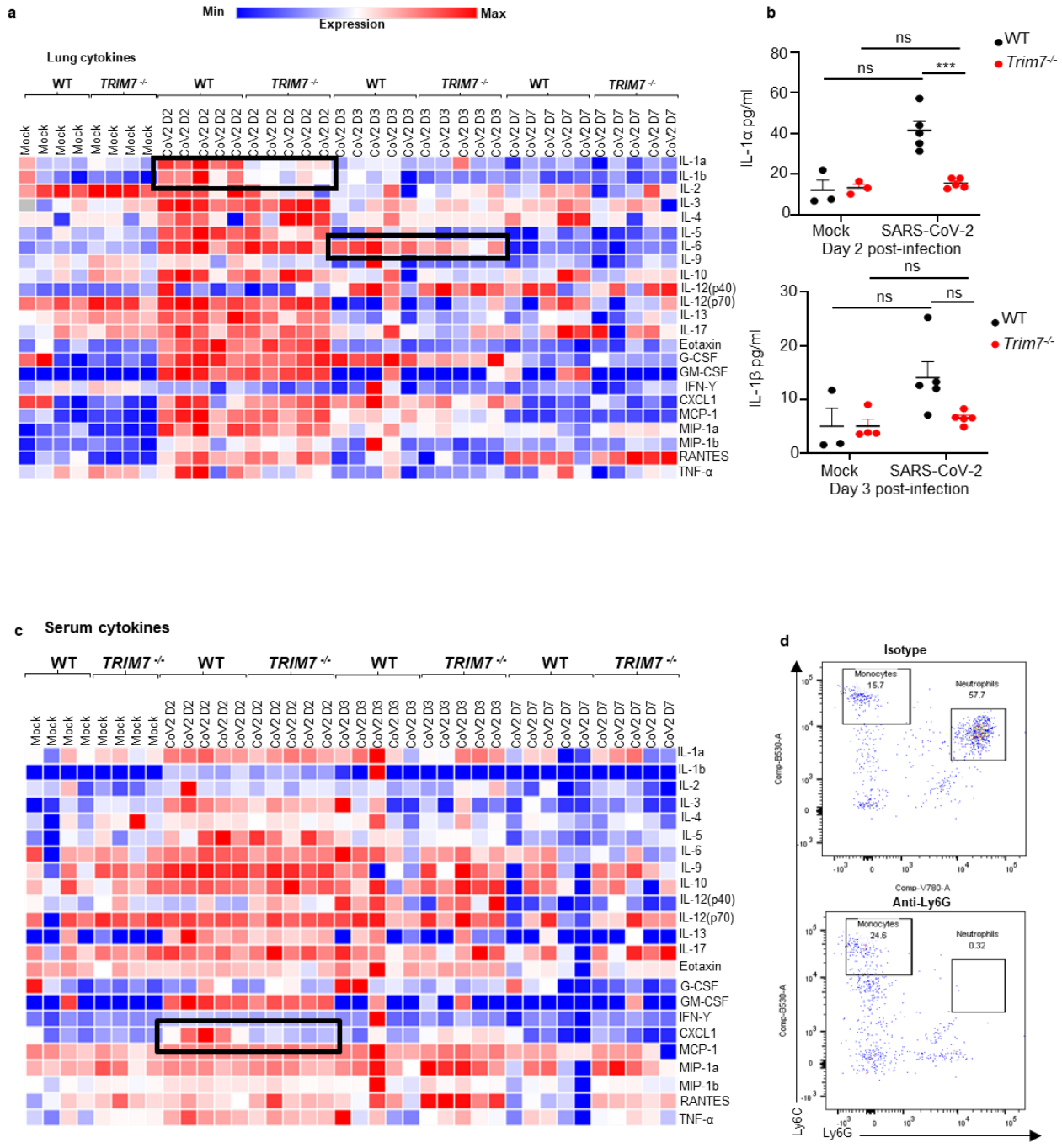

Figure S4. Multiplex analysis of lung homogenates and serum. a) heat map of cytokine expression in lung of infected mice. b) lung homogenate concentration levels ofIL-1α in lung of WT and *Trim7*$^{-/-}$ mice. c) heat map of cytokine expression in serum of infected mice. d) representative dot blot of peripheral blood staining showing depletion of neutrophils CD45^{+} CD11c^{-}CD11b^{+}Ly6C^{int}, Ly6G^{hi}. Data are depicted as Mean ± SEM. 2-way Tukey's multiple comparisons tests. $p < 0.001$ **, $p < 0.0001$ ***, $p < 0.00001$ ****.

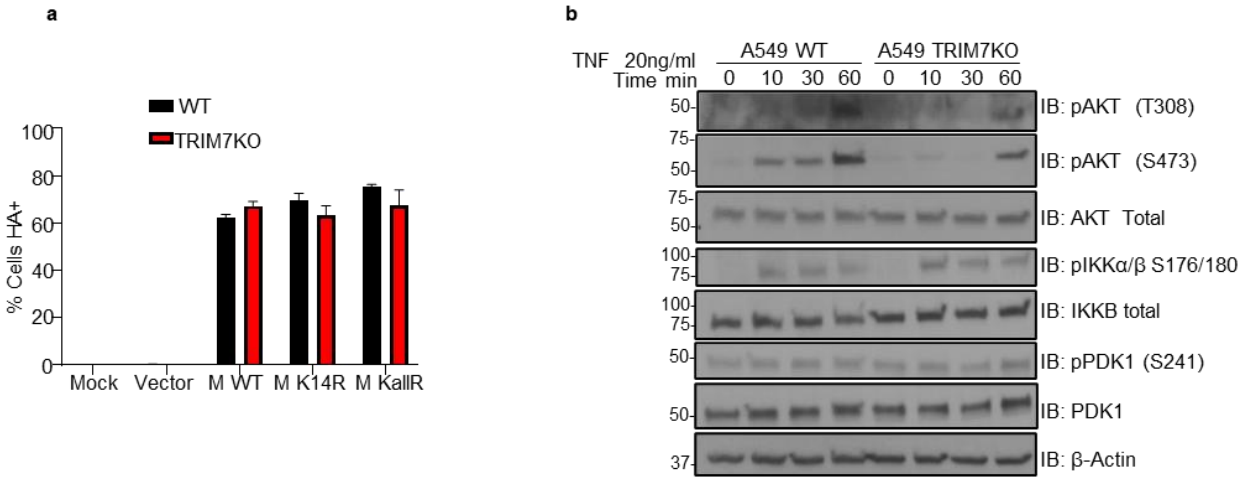

Figure S5. TRIM7KO cells have impaired activation of AKT pathway after TNF stimulation. a) frequency of cells transfected with M-WT, M-K14R and M-KallR. b) western blot of A549 WT and TRIM7 KO starved for 8h and then stimulated with 20ng/ml of TNF for 10, 30 and 60 minutes.

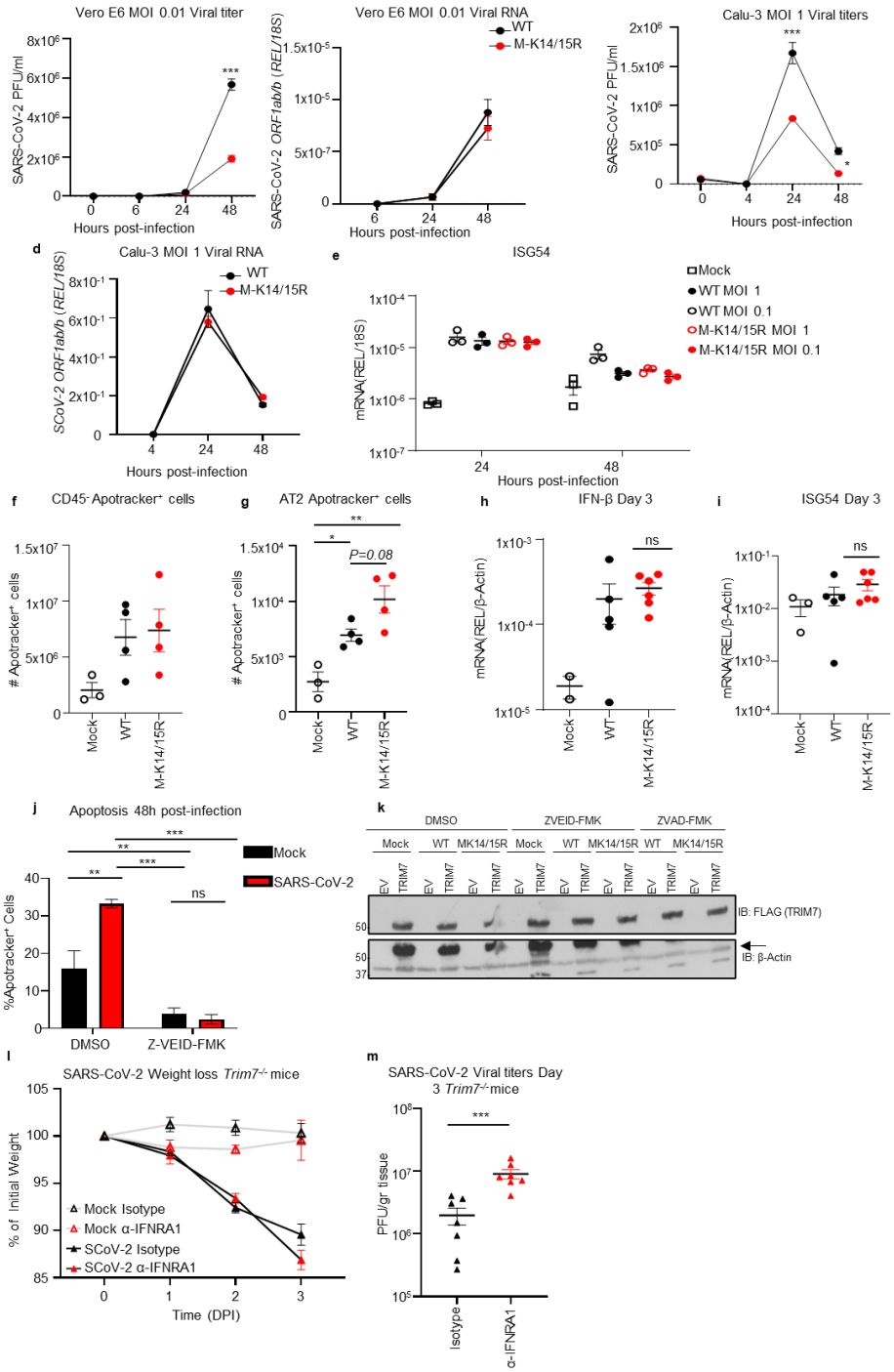

Figure S6. M-K14/15R virus has defective budding but no IFN response is affected. Vero E6 and Calu-3 infected with SARS-CoV-2 WT and M-K14/K15R MOI of 0.01 and 1 respectively. a) viral titers and b) viral RNA in Vero E6. c) viral titers and d) viral RNA in Calu-3. e) ISG54 expression in Calu-3 cells. WT mice infected with WT or M-K14/15R. f) lung CD45$^-$ cells Apotracker$^+$ and g) lung Alveolar Type 2 (AT2) cells (CD45$^-$ CD31$^-$ CD24$^-$ Podoplanin$^-$ EpCAM$^+$ MHC-II$^+$) positive for Apotracker staining. h) mRNA levels of IFN-β, and i) IS54. j) frequency of HEK 293T-hACE-2 cells infected with SARS-CoV-2 and treated with vehicle or 50μM of Z-VEID-FMK stained with Apotracker Green 48h post-infection. k) western blot analysis of expression of TRIM7-FLAG in 293T cells infected with CoV-2 WT and M-K14/K15R MOI 0.1 and treated with caspases inhibitors Z-VEID and Z-VAD. *Trim7*$^{-/-}$ mice treated with anti-IFNRA1 or isotype mock (n=3 males each group) at day 1 before infection and infected intranasal with SARS-CoV-2 CMA3p20 (n=7, 5 females and 2 males) for 3 days. l) weight loss and m) Viral lung titers. Data are depicted as Mean ± SEM. T-test analysis, one-way or 2-way Tukey's multiple comparisons tests. p < 0.001 **, p < 0.0001 ***, p < 0.00001 ****.

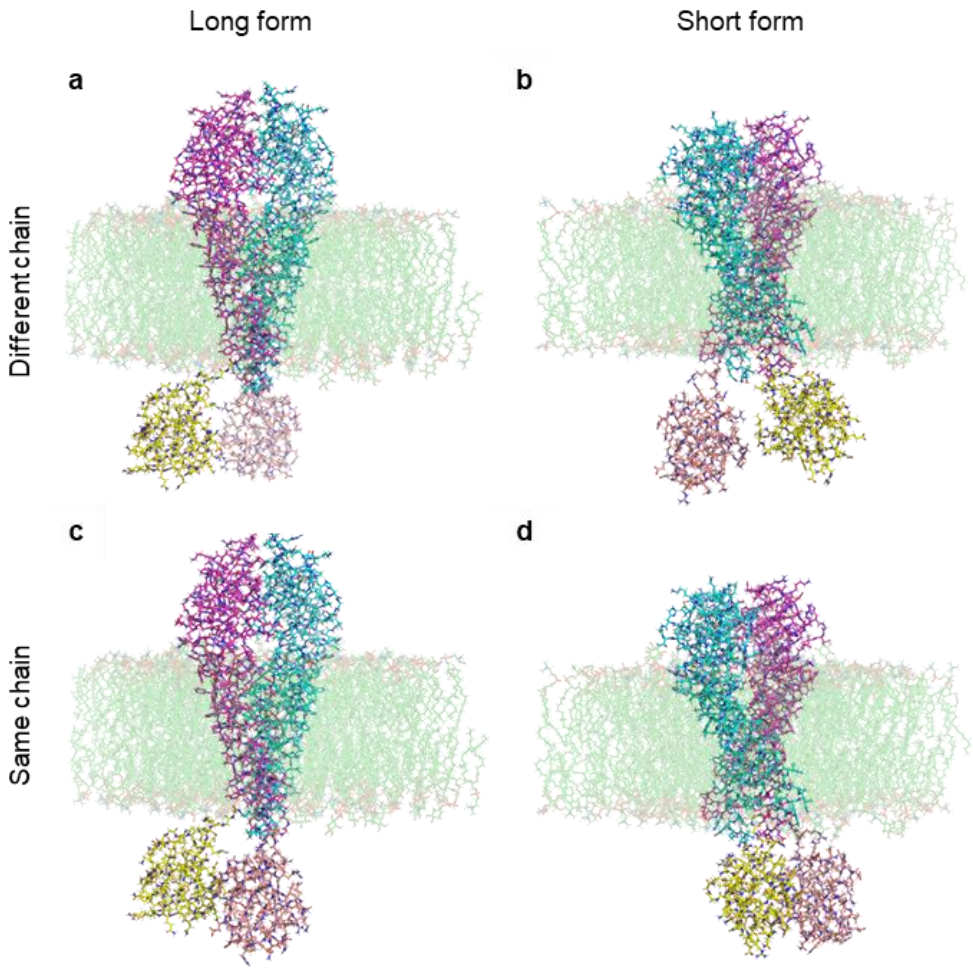

Figure S7. Structural modeling of M. Modeling of different possible ubiquitinated M dimers. The two chains of the M homodimer are shown in cyan and magenta whereas ubiquitin (Ub) is presented in yellow and salmon (the membrane is shown in green). a) long form of M (PDB 7VGR) with Ub attached to K14 and K15 in different chains. b) short form of M (PDB 7VGS) with Ub attached to K14 and K15 in different chains. c) long form of M with Ub attached to K14 and K15 in the same chain. d) short form of M with Ub attached to K14 and K15 of the same chain. Energetically based on the estimations with Surfaces, model A is the most favorable of the four, with full system ΔΔG calculations showing $\Delta\Delta G_{A\rightarrow B}$= 3.89 kcal/mol, $\Delta\Delta G_{A\rightarrow C}$= 1.01 kcal/mol, $\Delta\Delta G_{C\rightarrow D}$= 5.12 kcal/mol, and $\Delta\Delta G_{B\rightarrow D}$= 2.24 kcal/mol. In both cases (double ubiquitination in the same, or different chains), the long form is preferred.

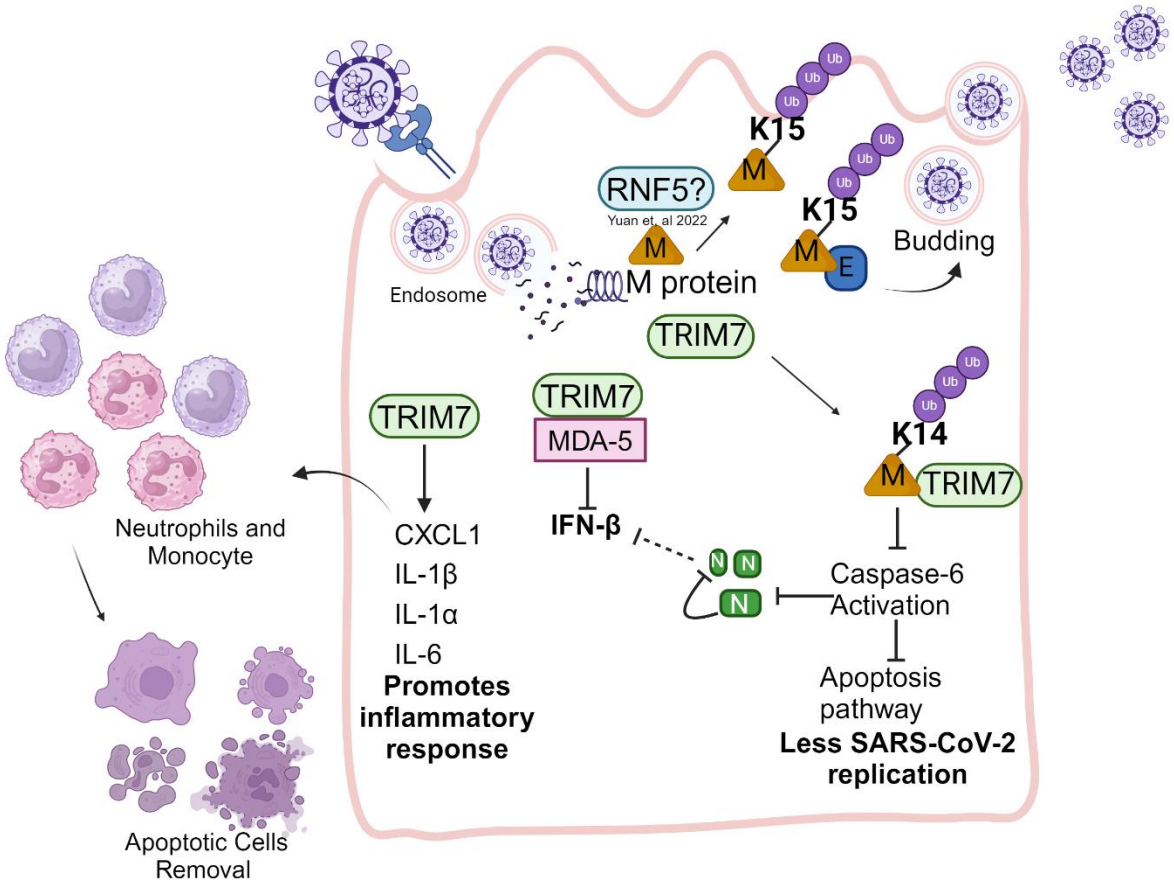

Figure S8. Multifunctional role of TRIM7 during SARS-CoV-2 infection. M protein can be ubiquitinated possibly by RNF5 on K15 residue, this is important for virus budding. On the other hand, TRIM7 can ubiquitinate M protein in the K14 residue, this ubiquitination is important to regulate caspase-6 activation and to inhibit apoptosis as well as to reduce the cleavage of N that could in turn inhibit the IFN-I production. TRIM7 can also interact with cytosolic receptor MDA-5 and inhibit the promoter activity of IFN-β by a mechanism that still unknown. TRIM7 is important to promote the production of pro-inflammatory cytokines IL-6, IL-1β and IL-1α as well as the chemokine CXCL1 that recruits neutrophils and monocytes to the lung, here these cells promote the removal of the apoptotic cells induced by SARS-CoV-2 and contribute with tissue repair. Created with BioRender.com.

Table 1. Mutations on Membrane protein K14 residue across clades.

Clade	Residue Mutation	Sample Mutation count	Total Samples in Clade	Clade mutation %	Total Mutations	Clade Total Mutations %
19A	K14del	113	11833	0.955	113	0.955
19B	K14del	11	7387	0.1489	11	0.149
20A	K14R	3	120679	0.0025	274	0.227
20A	K14E	1	120679	0.0008	274	0.227
20A	K14del	270	120679	0.2237	274	0.227
20B	K14R	3	104912	0.0029	137	0.131
20B	K14del	134	104912	0.1277	137	0.131
21A	K14E	2	53799	0.0037	2	0.004
20E	K14E	4	103929	0.0038	8	0.008
20E	K14del	4	103929	0.0038	8	0.008
20C	K14E	8	68701	0.0116	54	0.079
20C	K14F	1	68701	0.0015	54	0.079
20C	K14R	1	68701	0.0015	54	0.079
20C	K14del	44	68701	0.064	54	0.079
21H	K14E	5	6144	0.0814	5	0.081
21B	K14R	1	1045	0.0957	1	0.096
20I	K14*	1	651108	0.0002	23	0.004
20I	K14R	5	651108	0.0008	23	0.004
20I	K14Q	1	651108	0.0002	23	0.004
20I	K14E	5	651108	0.0008	23	0.004
20I	K14G	1	651108	0.0002	23	0.004
20I	K14del	7	651108	0.0011	23	0.004
20I	K14T	3	651108	0.0005	23	0.004
20D	K14del	9	6020	0.1495	9	0.15
21I	K14E	2	151093	0.0013	7	0.005
21I	K14R	1	151093	0.0007	7	0.005
21I	K14del	4	151093	0.0026	7	0.005
21J	K14I	8	2737780	0.0003	111	0.004
21J	K14R	15	2737780	0.0005	111	0.004
21J	K14Q	8	2737780	0.0003	111	0.004
21J	K14E	60	2737780	0.0022	111	0.004
21J	K14del	19	2737780	0.0007	111	0.004
21J	K14T	1	2737780	0	111	0.004
20H	K14R	14	9553	0.1466	16	0.167
20H	K14del	2	9553	0.0209	16	0.167
21F	K14R	1	33858	0.003	2	0.006
21F	K14del	1	33858	0.003	2	0.006

21C	K14E	1	41628	0.0024	1	0.002
21K	K14E	8	1591473	0.0005	70	0.004
21K	K14G	1	1591473	0.0001	70	0.004
21K	K14del	54	1591473	0.0034	70	0.004
21K	K14R	7	1591473	0.0004	70	0.004
21L	K14E	2	1143006	0.0002	57	0.005
21L	K14del	46	1143006	0.004	57	0.005
21L	K14T	5	1143006	0.0004	57	0.005
21L	K14R	4	1143006	0.0003	57	0.005
22D	K14Q	1	31187	0.0032	2	0.006
22D	K14R	1	31187	0.0032	2	0.006
22F	K14R	2	20443	0.0098	2	0.01
22C	K14R	1	170929	0.0006	4	0.002
22C	K14E	1	170929	0.0006	4	0.002
22C	K14G	1	170929	0.0006	4	0.002
22C	K14del	1	170929	0.0006	4	0.002
22B	K14E	4	781430	0.0005	57	0.007
22B	K14del	10	781430	0.0013	57	0.007
22B	K14R	43	781430	0.0055	57	0.007
23C	K14R	1	28556	0.0035	1	0.004
23A	K14E	1	161212	0.0006	3	0.002
23A	K14R	2	161212	0.0012	3	0.002
23B	K14R	2	31125	0.0064	2	0.006
23E	K14E	1	11253	0.0089	7	0.062
23E	K14R	6	11253	0.0533	7	0.062
22E	K14R	5	195894	0.0026	6	0.003
22E	K14del	1	195894	0.0005	6	0.003

Table 2. Table 1. Mutations on Membrane protein K15 residue across clades.

Clade	Residue Mutation	Sample Mutation count	Total Samples in Clade	Clade Individual mutation %	Total Mutations	Clade Total Mutation %
19A	K15*	3	11833	0.0254	4	0.034
19A	K15N	1	11833	0.0085	4	0.034
20A	K15M	2	120679	0.0017	19	0.016
20A	K15E	8	120679	0.0066	19	0.016
20A	K15S	3	120679	0.0025	19	0.016
20A	K15R	1	120679	0.0008	19	0.016
20A	K15del	5	120679	0.0041	19	0.016
19B	K15del	1	7387	0.0135	35	0.474
19B	K15R	34	7387	0.4603	35	0.474
20B	K15N	26	104912	0.0248	32	0.031
20B	K15R	2	104912	0.0019	32	0.031
20B	K15del	4	104912	0.0038	32	0.031
21A	K15N	7	53799	0.013	8	0.015
21A	K15E	1	53799	0.0019	8	0.015
20C	K15N	55	68701	0.0801	106	0.154
20C	K15R	50	68701	0.0728	106	0.154
20C	K15E	1	68701	0.0015	106	0.154
21H	K15N	1	6144	0.0163	1	0.016
20E	K15N	19	103929	0.0183	25	0.024
20E	K15T	1	103929	0.001	25	0.024
20E	K15R	2	103929	0.0019	25	0.024
20E	K15del	3	103929	0.0029	25	0.024
20J	K15Q	2	29088	0.0069	2	0.007
20I	K15M	7	651108	0.0011	102	0.016
20I	K15N	22	651108	0.0034	102	0.016
20I	K15E	26	651108	0.004	102	0.016
20I	K15T	1	651108	0.0002	102	0.016
20I	K15R	40	651108	0.0061	102	0.016
20I	K15del	6	651108	0.0009	102	0.016
20D	K15N	1	6020	0.0166	1	0.017
20D	K15del	1	6020	0.0166	1	0.017
21I	K15N	4	151093	0.0026	37	0.024
21I	K15Q	1	151093	0.0007	37	0.024
21I	K15E	24	151093	0.0159	37	0.024
21I	K15del	3	151093	0.002	37	0.024
21I	K15R	5	151093	0.0033	37	0.024
21J	K15N	2433	2737780	0.0889	2785	0.102
21J	K15Q	165	2737780	0.006	2785	0.102
21J	K15T	7	2737780	0.0003	2785	0.102
21J	K15R	123	2737780	0.0045	2785	0.102
21J	K15del	29	2737780	0.0011	2785	0.102
21J	K15M	11	2737780	0.0004	2785	0.102

21J	K15E	17	2737780	0.0006	2785	0.102
20H	K15del	2	9553	0.0209	3	0.031
20H	K15R	1	9553	0.0105	3	0.031
21F	K15del	1	33858	0.003	1	0.003
21C	K15N	1	41628	0.0024	1	0.002
20G	K15N	4	83603	0.0048	6	0.007
20G	K15R	2	83603	0.0024	6	0.007
21K	K15T	1	1591473	0.0001	166	0.01
21K	K15N	31	1591473	0.0019	166	0.01
21K	K15R	35	1591473	0.0022	166	0.01
21K	K15Q	22	1591473	0.0014	166	0.01
21K	K15del	55	1591473	0.0035	166	0.01
21K	K15M	6	1591473	0.0004	166	0.01
21K	K15E	16	1591473	0.001	166	0.01
21L	K15N	7	1143006	0.0006	71	0.006
21L	K15R	11	1143006	0.001	71	0.006
21L	K15del	52	1143006	0.0045	71	0.006
21L	K15E	1	1143006	0.0001	71	0.006
22D	K15N	5	31187	0.016	7	0.022
22D	K15R	2	31187	0.0064	7	0.022
22F	K15del	1	20443	0.0049	5	0.024
22F	K15N	1	20443	0.0049	5	0.024
22F	K15R	3	20443	0.0147	5	0.024
22C	K15N	1	170929	0.0006	7	0.004
22C	K15R	5	170929	0.0029	7	0.004
22C	K15del	1	170929	0.0006	7	0.004
22B	K15del	13	781430	0.0017	106	0.014
22B	K15N	6	781430	0.0008	106	0.014
22B	K15E	3	781430	0.0004	106	0.014
22B	K15R	79	781430	0.0101	106	0.014
22B	K15Q	5	781430	0.0006	106	0.014
22A	K15N	1	95899	0.001	1	0.001
23C	K15R	1	28556	0.0035	1	0.004
23A	K15N	4	161212	0.0025	11	0.007
23A	K15R	7	161212	0.0043	11	0.007
23B	K15del	1	31125	0.0032	1	0.003
23D	K15N	69	36429	0.1894	72	0.198
23D	K15Q	1	36429	0.0027	72	0.198
23D	K15R	1	36429	0.0027	72	0.198
23D	K15E	1	36429	0.0027	72	0.198
23E	K15R	7	11253	0.0622	7	0.062
22E	K15del	1	195894	0.0005	4	0.002
22E	K15M	1	195894	0.0005	4	0.002
22E	K15N	1	195894	0.0005	4	0.002
22E	K15R	1	195894	0.0005	4	0.002
23F	K15N	1	31861	0.0031	4	0.013

23F	K15Q	2	31861	0.0063	4	0.013
23F	K15R	1	31861	0.0031	4	0.013

Table 3. Table 1. Mutations on Membrane protein K14/K15 residue across clades.

Clade	Residue Mutation	Sample Mutation count	Total Samples in Clade	Clade mutation %	Total Mutations	Clade Total Mutations %
19B	K14del, K15del	1	11833	0.008	1	0.008
20A	K14del, K15del	4	120679	0.003	4	0.003
20B	K14del, K15del	2	104912	0.002	2	0.002
20I	K14del, K15del	6	651108	0.001	6	0.001
20D	K14del, K15del	1	6020	0.017	1	0.017
20E	K14del, K15del	3	103929	0.003	3	0.003
21I	K14del, K15del	3	151093	0.002	3	0.002
21J	K14del, K15del	19	2737780	0.001	19	0.001
20H	K14del, K15del	2	9553	0.021	2	0.021
21F	K14del, K15del	1	33858	0.003	1	0.003
21K	K14del, K15del	51	1591473	0.003	52	0.003
21K	K14R, K15Q	1	1591473	0	52	0.003
21L	K14del, K15del	45	1143006	0.004	45	0.004
22C	K14del, K15del	2	170929	0.001	2	0.001
22B	K14del, K15del	11	781430	0.001	11	0.001
22E	K14del, K15del	1	195894	0.001	1	0.001